33rd Annual International Conference of the IEEE EMBS
Boston, Massachusetts USA, August 30 - September 3, 2011

Highly Adaptive RF Excitation Scheme Based on Conformal Resonant CRLH Metamaterial Ring Antennas for 7-Tesla Traveling-Wave Magnetic Resonance Imaging

Daniel Erni, *Member, IEEE*, Thorsten Liebig, Andreas Rennings, Norbert H. L. Koster, and Jürg Fröhlich

***Abstract* — We propose an adaptive RF antenna system for the excitation (and manipulation) of the fundamental circular waveguide mode (TE_{11}) in the context of high-field (7 T) traveling-wave magnetic resonance imaging (MRI). The system consists of «flat» composite right-/left-handed (CRLH) metamaterial ring antennas that fully conforms to the inner surface of the MRI bore. The specific use of CRLH metamaterials is motivated by its inherent dispersion engineering capabilities, which is needed when designing resonant ring structures for virtually any predefined diameter operating at the given Larmor frequency (i.e. 298 MHz). Each functional group of the RF antenna system consists of a pair of subsequently spaced and correspondingly fed CRLH ring antennas, allowing for the unidirectional excitation of propagating, circularly polarized B_1 mode fields. The same functional group is also capable to simultaneously mold an incoming, counter-propagating mode. Given these functionalities we are proposing now a compound scheme (i.e. periodically arranged multiple antenna pairs) – termed as "MetaBore" – that is apt to provide a tailored RF power distribution as well as full wave reflection compensation virtually at any desired location along the bore.**

I. Introduction

THE distribution of the RF B_1-field in the form of circularly polarized traveling waves being guided within the proper bore of the high-field (7T) MRI scanner has been proposed by Brunner et al. in their seminal publications [1], [2]. In the following many research groups have been inspired by this concept because it provides a potential measure for large field-of-view (FOV) imaging due to the resulting uniform field illumination at considerably high magnetic field strengths [2], [3]. Further research has thus focused on the proper delivery of traveling waves to the whole body using e.g. "coax-like" conducting extensions [4]. Recently, multiple dielectric extensions have been introduced on the front side section of the bore to enable RF shimming together with parallel transmit operation, while exploiting the emerging multimode nature of the pervaded waveguide section [5]. A common feature of all these approaches is a waveguide mode excitation that relies on a closed-end antenna system at the corresponding bore end, defining thus a quite challenging environment in terms of patient's comfort. In [6] we have therefore proposed an RF antenna system that could be fully concealed behind the bore housing, leaving the whole bore site unaltered. Such ergonomic advantage owes mainly to the conceptual flexibility of planar composite right-/left-handed (CRLH) electromagnetic metamaterials (cf. e.g. [7]-[12]) since their capability for true dispersion engineering offers an additional degree of design freedom.

II. CRLH Ring Antenna

A. Starting from linear CRLH metalines

The generic structure of the CRLH metamaterial is shown in Fig. 1. It consists of a unit cell that is periodically continued to form a one-dimensional (1D) so-called CRLH metaline. Similar to common transmission lines the CRLH metaline supports standing waves (of the order up to the number of involved unit cells) when either short- or open-circuited at both ends. The most peculiar resonant state is the zeroth-

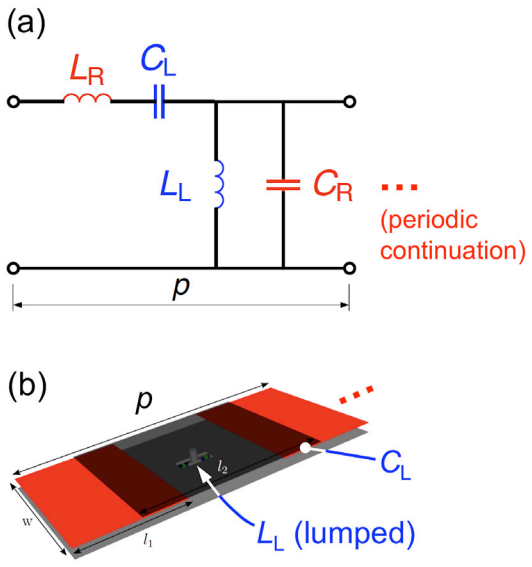

Fig. 1: Unit cell of the resonant CRLH metaline: (a) Equivalent electrical circuit of the unit cell with L_L and C_L being the elements of the left-handed contribution (blue), whereas L_R and C_R are representing the conventional (i.e. right-handed) transmission line elements (red). The quantity p stands for the footprint (i.e. periodicity) of the unit cell. (b) Metal-insulator-metal (MIM) multilayer realization of the unit cell (top, intermediate and bottom metal layers are displayed in black, red and grey) where the shunt inductor L_L is introduced as a lumped (or chip) element [9], [12].

Manuscript received April 14, 2011.

D. Erni, T. Liebig, A. Rennings, and N. H. L. Koster are with General and Theoretical Electrical Engineering (ATE), Faculty of Engineering, University of Duisburg-Essen, and CeNIDE – Center for Nanointegration Duisburg-Essen, D-47048 Duisburg, Germany (fax: +49(0)203/379-3499; e-mail: daniel.erni@uni-due.de; web: http://www.ate.uni-due.de).

J. Fröhlich, is with the Laboratory for Electromagnetic Fields and Microwave Electronics, ETH Zürich, CH-8092 Zürich, Switzerland (e-mail: j.froehlich@ifh.ee.ethz.ch).

order resonance (ZOR) represented by the singular non-vanishing transition frequency at $k=0$ for a *balanced* unit cell where the series resonance $1/\sqrt{(L_R C_L)}$ is matched to the shunt resonance $1/\sqrt{(L_L C_R)}$. The ZOR yields a *non-local* response, namely a uniform current or voltage distribution along the metaline depending on the type of the chosen mismatch (short or open circuit), where the former case is very attractive for providing uniform transversal B_1 fields in MRI scanners. The application of ZOR CRLH metalines for advanced coil designs in high-field MRI has been pioneered by Rennings et al. [7], and already proven successful for very large FOV [8] because the latter is likely to scale up according to the length of the linear structure (metaline) [9]. CRLH metalines can function as transmit/receive coils [10] and they are inherently *dual-band* (when unbalanced or operated at higher order resonances [11]), which is promising especially for functional (X-nuclei + 1H) MRI applications.

B. Conformal CRLH ring topologies

CRLH ring antennas simply evolve from the finite periodic array of unit cells (cf. Fig. 1) where both ends are then bent around to form a circle (cf. Fig. 2). From the periodic boundary conditions being enforced at these ends to ensure continuity of the fields in the proper joint, we can easily read off the resonant behavior of the ring topology, fostering e.g. dual-band full-wave resonances, where these two resonances are according the frequency gap between the right- and left-handed branch, respectively, of the dispersion diagram [11], [12]. The design of the CRLH ring antenna follows a two-stage approach, which starts with the equivalent circuit of the unit cell [cf. Fig. 1(a)] to determine the circuit elements L_L, C_L, L_R and C_R, as well as the number of unit cells for the given circumference and operation frequency (298 MHz) [13]. It is worth mentioning that the structure can even be simplified if we let $L_L \to \infty$ [i.e. neglecting the lumped shunt inductor in the unit cell as depicted in Fig. 1(b)] to get rid of the left-handed dispersion branch, having only a minor effect on the remaining "right-handed" operating band. This prior circuit analysis is then paralleled with full-wave EC-FDTD [14] simulations to obtain the proper geometrical dimensions of the unit cell [13]. Given the bore diameter of 64 cm and the top / intermediate / bottom metal layer, which encompass a spacing of 1.28 mm followed by 1 cm, where the upper two layers are part of a Rogers 3010 substrate ($\varepsilon_r = 10.2$) and the lower spacing is filled with air, the "degenerated" CRLH ring antenna has 32 unit cells with $p = 62.83$ mm ($\Leftrightarrow 11.25°$) and a width of 37 mm (extracted). From further extraction we get the gap width that amounts to 8.73 mm. The resulting length of the intermediate metal layer is therefore 62.83 mm − 8.73 mm = 54.10 mm. Increasing accuracy has been achieved through minor corrections stemming from the equivalent circuit finite-difference time-domain (EC-FDTD) full-wave analysis of the overall ring topology. The feeding of the ring antenna is easy to implement just by driving either the top or the intermediate metal layer of a corresponding unit cell against the bottom layer at positions (modulo one unit cell) using e.g. a voltage source. The flexibility in the feeding position is advantageous if e.g. symmetry constraints have to be met such as in the case of quadrature excitation to obtain a *rotating* current distribution as depicted in Fig. 2.

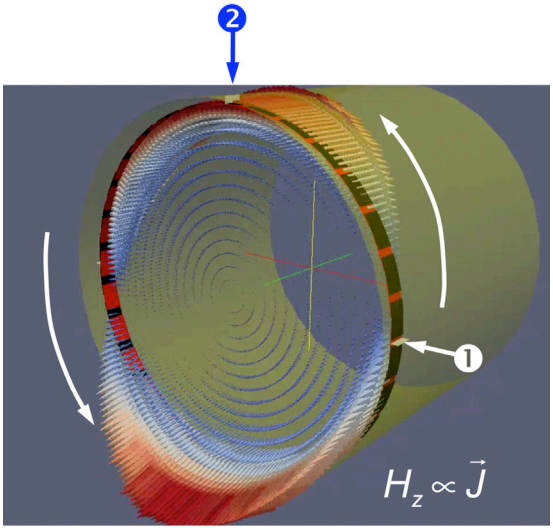

Fig. 2: The concatenated unit cells of Fig. 1(b) are bent around to form a (conformal) resonant CRLH ring antenna. The picture shows an EC-FDTD simulation of the H_z field component, and hence the current density $\boldsymbol{J}$ on the surface along the ring structure at full-wave resonance (298 MHz). The CRLH ring antenna consists of 32 elements (i.e. unit cells) that conform the inner surface of the MRI bore (∅ = 64 cm). The scheme allows the simple implementation of a quadrature excitation (with ① having an excitation phase of φ, and ② of φ − 90°) yielding a counter-clockwise rotating current distribution (as indicated).

It's worth emphasizing that the current distribution along the ring antenna perfectly coincides with the surface currents of the TE_{11}-mode within a circular hollow waveguide (i.e. the bore) rendering the CRLH ring topology an efficient scheme for the excitation of (two counter-propagating!) traveling waves.

C. Unidirectional wave excitation with ring antenna pairs

Multiple ring antennas being considerably grouped along the bore are prerequisite for obtaining single *unidirectional* wave excitation with any desired amplitude and phase origin [6]. The smallest set that yields this functionality is a pair of ring antennas separated by the distance d. The conditional equation for generating a forward propagating wave J^+ is then given below

$$J_1 + J_2 \cdot \exp\left\{ j\left(-2\beta d + \varphi_{12}\right)\right\} = 0$$

$$\Rightarrow \left| \begin{array}{ll} J_1 = J_2 & \\ \varphi_{12} = \beta d + (2n-1)\pi & \forall\, n \in \mathbb{N} \end{array} \right. \qquad (1),$$

where J_1 stands for the current excitation in the first antenna, J_2 is the corresponding excitation in the second antenna (located further apart in propagation direction), having a phase angle of φ_{12} with reference to J_1, and β represents the phase constant of the TE_{11}-mode in the (yet still unperturbed) bore.

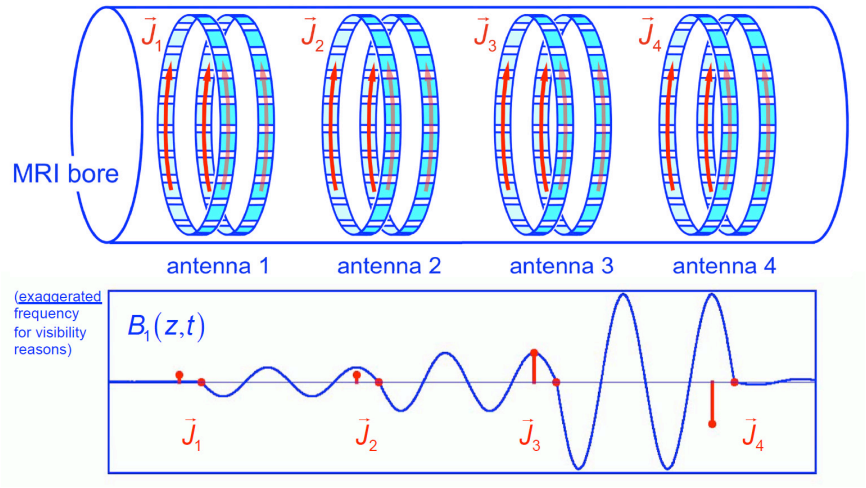

Fig. 3: Generic topology of the adaptive traveling-wave excitation system consisting of multiple pairs of resonant CRLH ring antennas (top). Temporal snapshot of the B_1 field along the bore axis (the frequency has been exaggerated for visibility reasons) together with the excitation currents $\boldsymbol{J}_i$ in the corresponding antenna pairs (bottom): Antenna (pair) #1 is used for unidirectional wave excitation (from left to right), whereas antenna #2 and #3 are used for coherent wave amplification, and with antenna #4 the traveling wave is actively dumped using destructive interference [6]. It's worth remembering that the magnetic field of the resulting traveling wave $B_1(z,t)$ is directly related to the behavior of the corresponding surface current density J^+.

Using the current and phase relation indicated in eqn. (1) yield thus a forward propagating unidirectional wave with the surface current amplitude according to

$$\left|J^+\right| = J_1 \cdot \left|1+\exp\left\{j\left(2\beta d-\pi\right)\right\}\right| \qquad (2).$$

The most economic case in terms of excitation amplitudes is $d=\lambda/4$ and $\varphi_{12}=-\pi/2$, where $J^+=2J_1$; meaning that smaller distances d require larger excitation amplitudes $J_{1,2}$ to maintain the same level of wave amplitude J^+.

A challenging issue that requires careful attention concerns the input impedance $\underline{Z}_{in}$ at the antenna feed. At resonance $\underline{Z}_{in}$ strongly deviates from half the Bloch impedance to reach values in the order of 300 Ω. Hence, to achieve power matching the source impedance has to conform this value too. But regarding an impinging TE_{11}-wave the ring antenna becomes only "transparent" for small $\underline{Z}_{in}$, namely if the feed is virtually short-circuited. Currently we are investigating voltage source driven feeding partly at intermediate impedance levels, and the use of lumped element circulators to separate the two distinct matching tasks.

III. The "MetaBore"

A. Working principle

The discussed CRLH ring antenna pairs can now be used as building blocks to setup an adaptive traveling-wave excitation system as depicted in Fig. 3. Relying on the superposition of fields (or sources), the antenna pairs are consecutively arranged along the bore (or intertwined accordingly) to form the so-called "MetaBore". Here the circularly polarized TE_{11}-wave is excited, (re-) amplified while adding a corresponding unidirectional constructively interfering partial TE_{11}-wave, or actively dumped in the vicinity of the bore opening when interfering with an identical but negatively weighted TE_{11}-wave (cf. Fig. 3). In addition, the underlying framework of the "MetaBore" also allows for the introduction of local phase shifts into the traveling TE_{11}-wave train, as well as the implementation of locally confined resonant standing wave regimes. The most flexible "MetaBore" topology with respect to the aforementioned functionalities therefore consists of periodically arranged ring antennas as e.g. depicted in Fig. 4.

B. Numerical simulations

Our numerical full-wave simulations rely on the equivalent-circuit (EC) finite-difference time-domain (FDTD) method [14], which has already proven successful for handling highly dispersive material (and device) properties [15] in the time-domain. In order to conform to the specific bore geometry we developed a cylindrical EC-FDTD implementation with sub-gridding capabilities [16]. The primary release already yields a numerical performance of around 300 Mcells/s/CPU on an Intel Core-i7 and a MPI version for cluster computing is on the way. We also "re-sampled" the surface-based anatomical model of a male adult from the *Virtual Family*™ [17] to enable future dosimetric assessment in the framework of our cylindrical implementation.

C. Proof-of-concept

A first evaluation of the proposed "MetaBore" concept has been carried out numerically, while analyzing the multi-ring antenna setting as described in Fig. 4. The bore length is assumed to be 3 m, where the antenna spacing amounts to 20 cm, which makes the overall antenna system to consist of 15 "degenerated" CRLH ring antennas each with 32 unit cells. The spacing of the ring antennas has to be chosen care-

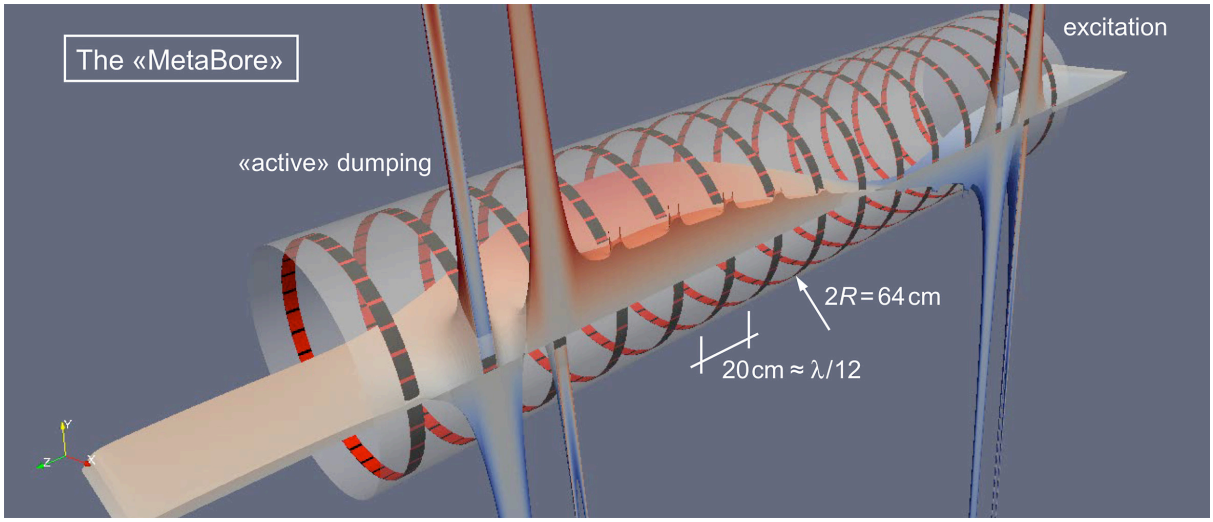

Fig. 4: Proof-of-concept: Cylindrical EC-FDTD full-wave simulation of the "MetaBore" at 298 MHz including 15 CRLH ring antennas each having 32 unit cells. For clarity reasons the figure shows the E_r component (instead of the transversal B_1-field) in the x-z-plane of the circularly polarized, propagating TE_{11}-mode (from right to left). This representation thus allows also to display the electrical field strength at the proper feedings of the active ring antenna pairs (cf. peaks), where unidirectional wave excitation takes place in the vicinity of the rear end of the bore, and the "active wave dumping" is effective at the front-end.

fully because the periodic loading of the bore actually constitutes a different eigenvalue problem fostering a TE_{11}-like Bloch wave with a 8 MHz higher cutoff frequency compared to the cutoff at 274 MHz of the TE_{11}-mode in the bare bore. This detuning yields an increase of the guided wavelength at 298 MHz in the order of 90 cm, rendering the amplitude condition in eqn. (2) slightly more challenging.

The analyzed scenario demonstrates the locally confined (along the propagation direction) unidirectional wave excitation at the far-end of the bore together with the successful active dumping at the near-end for an operating frequency of 298 MHz. These excitations have been made visible by displaying the dominant electric field component instead of the magnetic field within a plane that intersects one of the quadrature feeds in each antenna. The simulation time for a full-wave cycle amounts to 15 h on a state-of-the-art PC (Core-i7).

IV. Conclusion and Outlook

Within the presented feasibility study we have proven that the conformal CRLH ring antennas are best suited as building blocks to setting up a highly adaptive RF antenna system (i.e. the "MetaBore") for the excitation and molding of propagating TE_{11}-waves along the bore of a high-field MRI scanner. One of the most innovative aspects of our approach lies in the flexible form factor offered by the chosen CRLH antenna element, allowing the "MetaBore" to be totally concealed behind the bore housing while leaving the bore volume fully accessible for any clinical diagnostic purpose.

To further explore the functionality of the "MetaBore" we are currently investigating *adjustable power distributions* to e.g. relax safety issues [cf. Fig. 5(b)], and the compensation of wave reflections at distinct axial inhomogeneities appearing e.g. in the shoulder-neck area [cf. Fig. 5(c)].

The *active reflection compensation* uses a single narrowly spaced (e.g. $d = 0.03\ldots0.08\cdot\lambda$) ring antenna pair in the very vicinity of the inhomogeneity. To give an illustrative example: When assuming an incident wave J^+ that is reflected (and transmitted) at an air-dielectric interface with $\Delta\varepsilon_r = 3$, the first current set J_1 and J_2 (each of which is conceptualized as quadrature excitation) to be impressed into the ring antenna

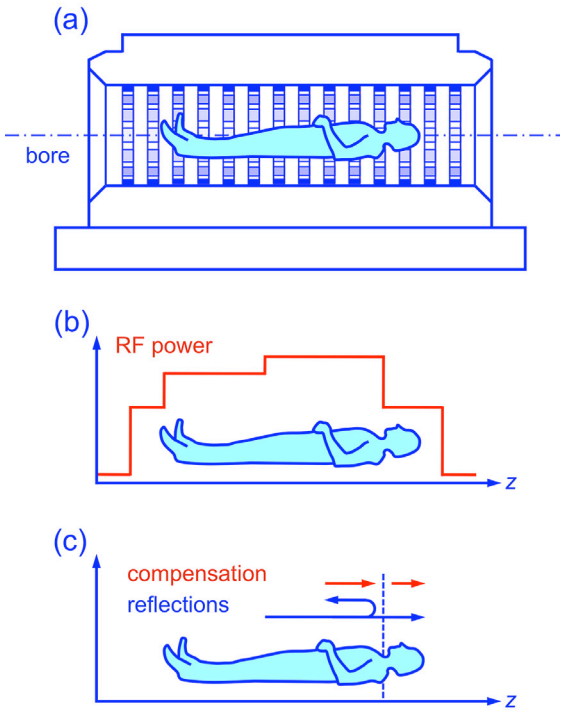

Fig. 5: Functionality of the "MetaBore": (a) Schematic of the correspondingly upgraded MRI scanner. (b) Tailoring the axial RF power distribution. (c) Reflection compensation scheme at e.g. the neck-shoulder inhomogeneity.

pair goes for the completion of the forward transmitted wave, whereas a second current set J_1^* and J_2^* is super-imposed to compensate the (backward) reflection of both, the incident wave and the forward wave stemming from the first set J_1 and J_2. In this particular example the resulting two current excitations $J_1 + J_1^*$ and $J_2 + J_2^*$ of the CRLH ring antenna pair amounts each to $1.3 \cdot J^+$.

We are investigating now excitation concepts where the currents J_i of *all* ring antennas become subject to optimization in order to meet tailored axial profiles (cf. Fig. 5) with respect to e.g. RF power or mode amplitudes of (circularly polarized) forward and backward propagating B_1 fields, together with the corresponding SAR measures. In addition to this longitudinal control scheme, *RF shimming* for transversal slice-selective excitation might be in principle accessible too, where transversal spatial field patterns are addressed with the corresponding superposition of various *elliptically* polarized and phase-related TE_{11}-mode fields that could be excited within the same antenna as depicted in Fig. 2. Taking into account the encoding ability of the gradient trajectory leads us then to the parallel transmit (pTX) scheme. Whether pTX can mitigate emergent variations in local SAR while keeping up with a desired B_1 profile is still lively debated [19]. The feasibility of parallel MRI in traveling-wave schemes using the diversity of multimode excitation is discussed in [5].

Our future research will also explore the appropriateness of the "MetaBore" for the *receive* operation. Due to the large antenna volume SNR issues are becoming increasingly important, not to mention the specific context of the traveling-wave scheme. A successful validation should therefore include RF receive fields stemming from appropriate material models [17], [18] that are capable to track down the magnetization of the spin system, where the latter may be represented as an auxiliary Bloch equation in the framework of our EC-FDTD scheme.

When looking at the overall antenna system in Fig. 4 we notice that with a guided wavelength of around 2.6 m…3.5 m the topology even fulfills the metamaterial criterion $\lambda >> p$ with respect to the propagation direction, making the proposed "MetaBore" a true two-dimensional (2D) cylindrical metamaterial (i.e. a meta-surface). Within this research agenda we therefore hope to reveal the "MetaBore" as a *holistic* approach to the realization of multi-functional traveling-wave MRI.

ACKNOWLEDGMENT

D. E. and J. F. kindly acknowledge fruitful discussions with Klaas Prüssmann on the potential of conformal (as well as ergonomic) excitation schemes in traveling-wave MRI.

REFERENCES

[1] D. O. Brunner, N. De Zanche, J. Paska, J. Fröhlich, and K. P. Pruessmann, "Travelling-wave MR: Comparison with a volume resonator at 7T," *ESMRMB 2008,* 25th Ann. Sci. Meeting, Oct. 2-4, Valencia, Spain, Paper 91, pp. 61-62, 2009.

[2] D. O. Brunner, N. De Zanche, J. Fröhlich, J. Paska, and K. P. Pruessmann, "Travelling-wave nuclear magnetic resonance," *Nature*, vol. 457, pp. 994-998, Feb. 2009.

[3] D. O. Brunner, J. Paska, J. Fröhlich, and K. P. Pruessmann, "Travelling-wave MRI: Initial results of in-vivo head imaging at 7T," *Proc. Intl. Soc. Mag. Reson. Med., 17th Sci. Meeting & Exhibition*, April 18-24, Honolulu, Hawaii, pp. 499, 2009.

[4] A. Andreychenko, D. W. Klomp, B. van den Bergen, B. L. van de Bank, H. Kroeze, J. J. Lagendijk, P. Luijten, and C. A. van den Berg, "Effective delivery of the traveling wave to distant locations in the body at 7T," *Proc. Intl. Soc. Mag. Reson. Med. 17th Sci. Meeting & Exhibition*, April 18-24, Honolulu, Hawaii, pp. 500, 2009.

[5] D. O. Brunner, J. Paska, J. Fröhlich, and K. P. Pruessmann, "Traveling-wave RF shimming and parallel MRI" *Magn. Reson. Med.*, online first, Feb. 24, 2011.

[6] D. Erni, A. Rennings, N. H. L. Koster, T. Liebig, «Wanderwellen-Magnetresonanztomographie Antennenvorrichtungen (WW-MRT)», Universität Duisburg-Essen, Allgemeine und Theoretische Elektrotechnik (ATE), May 27, 2010, utility model, German patent office, reference number DE 20 2010 003 162 U1, together with a German patent application, (reference number 10 2010 010 189.3-54).

[7] A. Rennings, J. Mosig, A. Bahr, C. Caloz, M. E. Ladd, and D. Erni, "A CRLH metamaterial based RF coil element for magnetic resonance imaging at 7 Tesla," *3rd European Conference on Antennas and Propagation (EuCAP 2009)*, March 23-27, Berlin, Germany, Session Thu-P-4.57, pp. 3231-3234, 2009.

[8] A. Rennings, P. Schneider, C. Caloz, and S. Orzada, "Preliminary experiments on a CRLH metamaterial zeroth-order resonant coil (ZORC) element for 7 Tesla MRI applications with large field of view," *METAMATERIALS 2009*, Sept. 1-4, London, UK, Special Session 4, pp. 126-128, 2009. (invited paper)

[9] A. Rennings, P. Schneider, S. Otto, D. Erni, C. Caloz, and M. E. Ladd, "A CRLH zeroth-order resonant antenna (ZORA) with high near-field polarization purity used as an RF coil element for ultra high field MRI," *METAMATERIALS 2010,* Sept. 13-16, Karlsruhe, Germany, pp. 92-94, 2010. (invited paper)

[10] J. Mosig, A. Bahr, T. Bolz, and A. Rennings, "Design and characteristics of metamaterial transmit/receive coil element for 7 Tesla MRI," *World Congress 2009 on Medical Physics and Biomedical Engineering (WC 2009)*, Sept. 7-12, Munich, Germany, IFMBE Proc. 25/II, pp. 173-176, 2009.

[11] A. Rennings, S. Otto, T. Liebig, C. Caloz, and I. Wolff, " Dual-band composite right/left-handed ring antenna with linear/circular-polarization capability," *1st Europ. Conf. On Antennas and Propagation (EuCAP 2006)*, Nov. 6-10, Nice, France, Session OA7, Paper 363935, 2006.

[12] Hui Wu, *Compact excitation and matching concepts for the travelling-wave nuclear magnetic resonance imaging (TW-MRI)*. Master thesis, Lab for General and Theoretical Electrical Engineering (ATE), University of Duisburg-Essen, Jan. 2010.

[13] T. Liebig, A. Rennings, S. Held, and D. Erni, "Accurate parameter extraction of lossy composite right/left-handed (CRLH) trans-mission lines for planar antenna applications," *METAMATERIALS 2010*, Sept. 13-16, Karlsruhe, Germany, pp. 456-458, 2010.

[14] Andreas Rennings, *Elektromagnetische Zeitbereichssimulationen innovativer Antennen auf Basis von Metamaterialien.* PhD Thesis University of Duisburg-Essen, Sept. 17, 2008,

[15] A. Rennings, J. Mosig, C. Caloz, D. Erni, and P. Waldow, "Equivalent circuit (EC) FDTD method for the modelling of surface plasmon based couplers," *J. Comput. Theor. Nanosci.*, vol. 5, no. 4, pp. 690-703, April 2008.

[16] T. Liebig, *openEMS*, a free and open computational electromagnetics platform based on EC-FDTD, University of Duisburg-Essen, available soon at: http://www.openems.de.

[17] A. Christ, W. Kainz, E.G. Hahn, K. Honegger, M. Zefferer, E. Neufeld, W. Rascher, R. Janka, W. Bautz, J. Chen, B. Kiefer, P. Schmitt, H.-P. Hollenbach, J. Shen, M. Oberle, D. Szczerba, A. Kam, J.W. Guag, and N. Kuster. "The Virtual Family – development of surface-based anatomical models of two adults and two children for dosimetric simulations," *Phys. Med. Biol.*, 55 N23-N38, Jan. 2010, (online Dec. 2009, http://dx.doi.org/10.1088/0031-9155/55/2/N01).

[18] S. Huclova, D. Erni, and J. Fröhlich "Modelling effective dielectric properties of materials containing diverse types of biological cells," *J. Phys. D: Appl. Phys.*, vol. 43, no. 36, pp. 365405–1-10, Sept. 15, 2010.

[19] Lawrence L. Wald, Elfar Adalsteinsson, "Parallel transmit technology for high field MRI," *MAGNETOM Flash*, vol. 1, pp. 124-133, 2009.